

D. RADOSZEWSKA*, T. GORYCZKA**, M. ADAMCZYK[#], B. WODECKA-DUŚ*,
D. BOCHENEK*, L. KOZIELSKI*

INFLUENCE OF Sr²⁺ DOPANT ON MICROSTRUCTURE AND ELECTRIC PROPERTIES OF (Ba_{0.85}Ca_{0.15})(Zr_{0.1}Ti_{0.9})O₃ (BCZT) CERAMICS

The discovery of (Ba_xCa_{1-x})(Zr_yTi_{1-x})O₃ lead-free ceramics drawn a lot of attention to those novel materials because of their excellent piezoelectric properties. However, quite a little attention has been paid to other features of the material. This article reports a wide range of research, including composition, structure and microstructure, dielectric response and impedance spectroscopy in order to systematize and expand knowledge about this peculiar ceramics and strontium doping effect on its properties. In order to test that influence a series of samples with various strontium concentration, precisely the admixtures of 0.02, 0.04 and 0.06 mol% were prepared, as well as basic ceramics to compare obtained results.

Keywords: microstructure, Sr²⁺, electric properties, (Ba_xCa_{1-x})(Zr_yTi_{1-x})O₃

1. Introduction

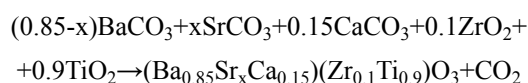
Recently lot of attention was given to unleaded ceramics due to the worldwide tendency to exclude heavy metals from the environment, and produce more eco-friendly materials. Among the others BaTiO₃ (BT) ceramics seems a good starting point for obtaining efficient material due to its relatively low Curie temperature ($T_C = 120^\circ\text{C}$) [1,2] and a great potential for application. There are variety of possibilities to change BT because of its isomorphism, but the solution provided by W. Liu and X. Ren [3] seems very promising, as the Ba(Zr_{0.2}Ti_{0.8})O_{3-x}(Ba_{0.7}Ca_{0.3})TiO₃ (BZT-xBCT) system they have obtained showed surprisingly good properties, especially for $x = 0.5$, which is near the morphotropic phase boundary (MPB). In hereby article Authors have decided to go a step further and additionally dope ceramics with strontium. Of course there already were attempts of doping that system with different ions, but neither the rare earth materials nor lanthanides, nor tantalum, iron or holm [4-10] had desired effect on the material. Thus we have decided to use strontium, as it is homovalent and it is expected to decrease T_C and preserve the shape of $\varepsilon(T)$, especially near its peak. Although the topic had been raised by Bai et al [11] further investigation had to be provided, especially as it comes to the impedance spectroscopy (IS).

In the present investigation (Ba_{0.85}Ca_{0.15})(Zr_{0.1}Ti_{0.9})O₃ (BCZT) ceramics was modified by an admixture of strontium in the amounts of 0, 0.02, 0.04 and 0.06 mol%, and the effects of doping on electrical properties of the obtained material was studied.

2. Materials and method

The described ceramics of the selected compositions were prepared using traditional mixed oxide (and carbonates) method, and the substrates for obtaining basic ceramics, as well as the doped one – (Ba_{0.85-x}Sr_xCa_{0.15})(Zr_{0.1}Ti_{0.9})O₃, were high purity (99.9%) strontium, barium, and calcium carbonates (SrCO₃, BaCO₃, CaCO₃) and zirconium and titanium oxides (ZrO₂, TiO₂).

All of the compounds were thoroughly weighted in a stoichiometric amounts according to the following chemical reaction:



for $x = 0, 0.02, 0.04$ and $0.06\text{mol}\%$. Then, prepared powders were milled for 24 h in a planetary mill, pressed into mouldings and synthesized. The conditions of synthesis were determined in accordance with thermal analysis and were set to $t = 2$ h at the temperature of $T_S = 950^\circ\text{C}$. Obtained materials were crumbled, milled and sieved and once more pressed into cylindrical mouldings and sintered for 4h at $T = 1450^\circ\text{C}$. The Archimedes displacement method with distilled water was conducted to evaluate the sample density. The bulk density of pure BCZT ceramics was 5.07 g/cm^3 but there is no simple relation between composition and value of the density, as for $x = 0.02, 0.04$ and 0.06 it has a value of $5.21, 4.65$ and 5.21 g/cm^3 respectively with average theoretical density of about 90%. After obtaining

* UNIVERSITY OF SILESIA, FACULTY OF COMPUTER SCIENCE AND MATERIAL SCIENCE, INSTITUTE OF TECHNOLOGY AND MECHATRONICS, 12 ŻYTANIA STR., 41-205 SOSNOWIEC, POLAND

** UNIVERSITY OF SILESIA, FACULTY OF COMPUTER SCIENCE AND MATERIAL SCIENCE, INSTITUTE OF MATERIALS SCIENCE, 75 PULKU PIECHOTY 1A, 41-500 CHORZOW, POLAND

Corresponding author: malgorzata.adamezyk-habrajska@us.edu.pl

the material a series of investigations has been done, including: microstructure examination, as well as element distribution, dielectric response and impedance spectroscopy (IS), described in the following section.

The microstructure of the discussed ceramics samples was analysed by a scanning electron microscope equipped with an energy dispersive X-ray spectrometer (EDS) with Si(Li) X-ray detector.

The obtained ceramics exhibit perovskite structure, which was confirmed by XRD measurements. XRD measurements were carried out on using PANalytical diffractometer X'Pert Pro with filtered $\text{Cu}_{K\alpha}$ radiation. The diffraction diagram was measured from 10° to 145° with 0.05° steps and a 2s counting time.

The computerised automatic system based on precision LCR meter Agilent E4980A was used to measure the temperature dependencies of permittivity as well as the impedance spectra. Ceramics samples prepared for dielectric measurements as well as IS were coated with silver electrodes, using an appropriate silver paste, without thermal treatment. After that investigated materials were deaged by thermal treatment to allow recombination and relaxation of the frozen defects, formed during the sintering process.

3. Results and discussion

3.1. Microstructure, EDS microanalysis and X-Ray Diffraction

The microstructure of strontium modified ceramics is illustrated on Fig. 1. An analysis of the results shown that the grain size decreases slightly with an increase of the dopant content. For the samples with strontium admixture of 0, 0.02 and 0.04 mol% grains are flat, well developed (their size is about $20\ \mu\text{m}$) and they have clearly defined boundaries, but for the last sample (0.06 mol%) it is visible that the ratio of smaller grains rises.

The distribution of all elements was investigated with Energy Dispersion X-ray spectrometer (EDS) and carried out for randomly selected areas. The analysis of the obtained data proved a homogenous distribution of elements throughout the grains and stoichiometry close to nominal.

The exemplary X-ray diffraction pattern (XRD) of BCZT ceramics obtained at room temperature is shown in Fig. 2.

The XRD profile was analysed and the materials were assigned to one phase – BaTiO_3 using ICDD PDF-2 database, but in all of the diagrams a presence of additional, yet not identified,

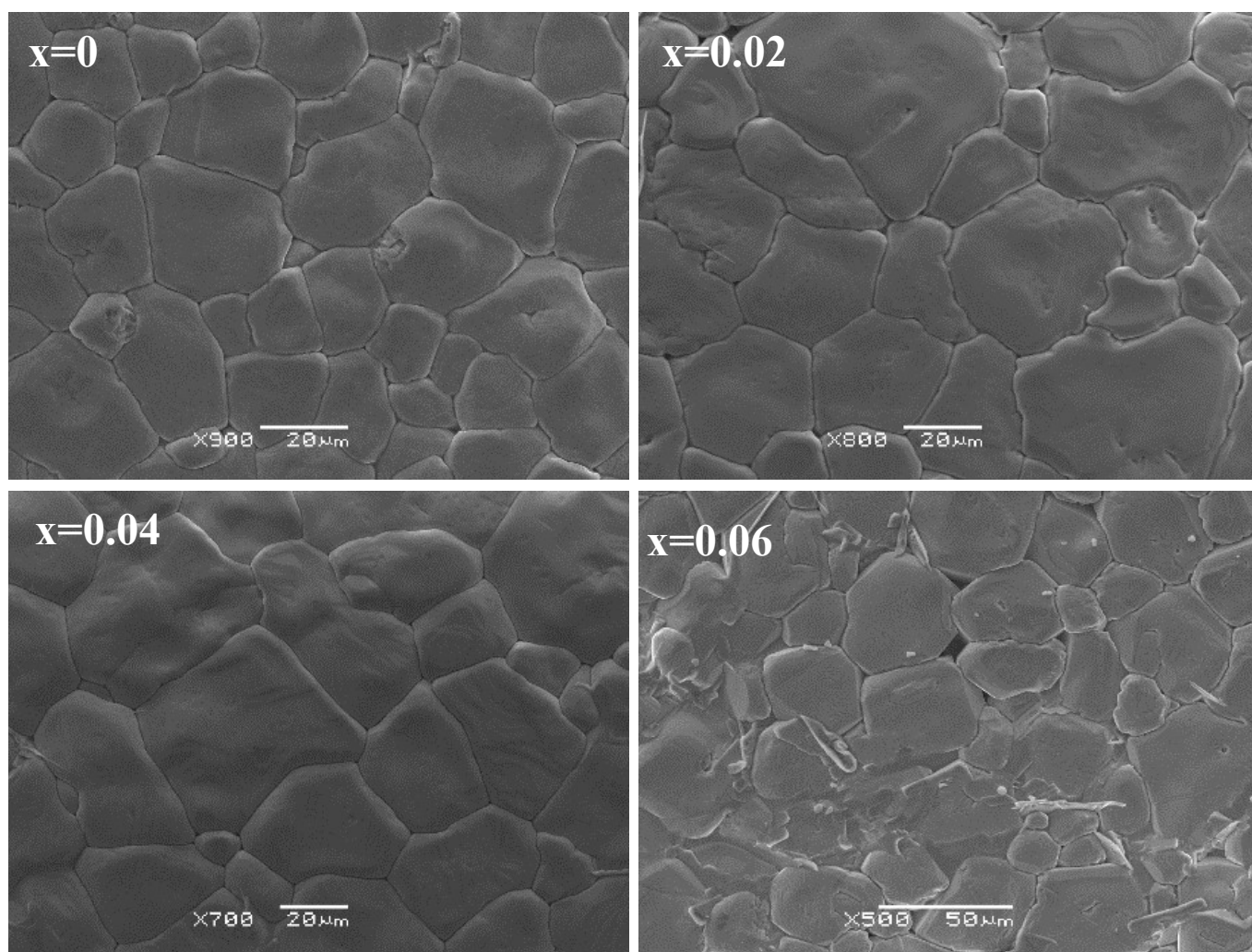


Fig. 1. SEM images of BCZT samples

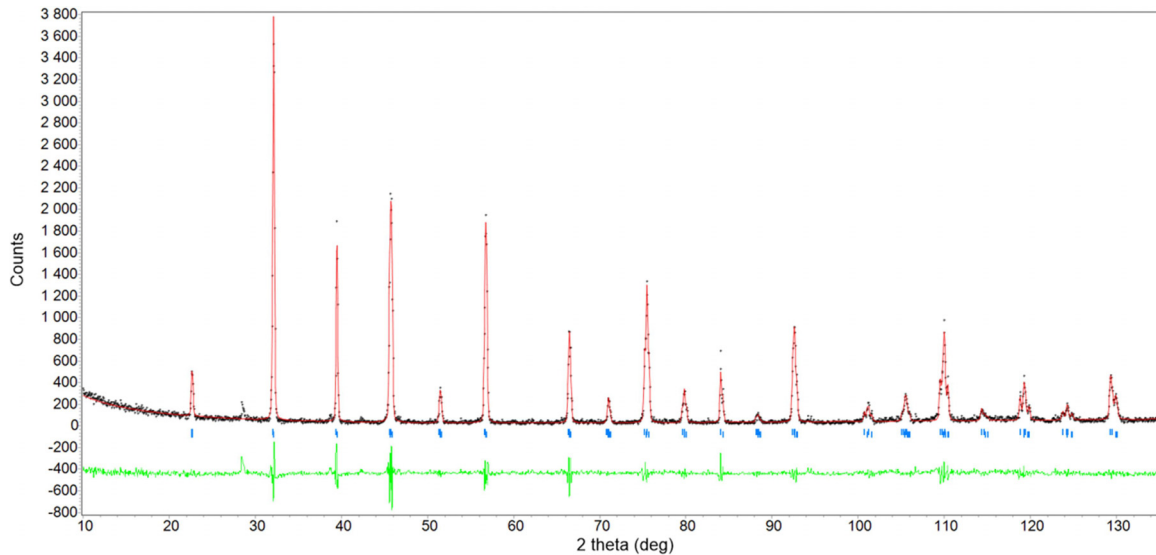


Fig. 2. An example of XRD pattern for sample with $x = 0.04$ mol%

phase can be observed at 28° , with an amount increasing with growing dopant concentration. The lattice parameters obtained from X-ray patterns are collected in Table 1.

TABLE 1
Lattice parameters obtained with XRD

	$x = 0$	$x = 0.02$	$x = 0.04$	$x = 0.06$
a_0 [Å]	4.000(0)	4.002(8)	4.000(3)	4.005(1)
b_0 [Å]	4.017(5)	4.018(2)	4.015(1)	4.012(4)

3.2. Dielectric response

The measurements of real (ϵ') and imaginary (ϵ'') parts of dielectric permittivity versus temperature were performed at frequencies in the range of 20 Hz-1 MHz. Temperature characteristics of dielectric response for 1kHz of without additives and strontium modified ceramics are shown in Fig. 3.

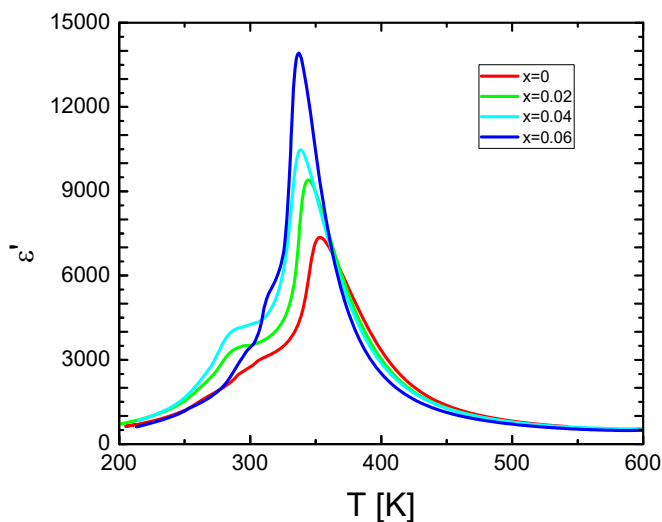


Fig. 3. Temperature dependence of dielectric permittivity measured at frequency of measuring field equal to 1 kHz

As it can be clearly seen, the rise of the dopant concentration leads to the increase of the dielectric permittivity peak value, with a simultaneous shift of the corresponding temperature to lower values. Moreover this process is approximately linear, both for dielectric permittivity maximum and temperature, what is typical for BT-based material, called “grain size effect” and widely described in literature [12-15]. However obtained ceramic materials show very small temperature hysteresis (about 4K), they do exhibit hysteresis as it comes to maximum of dielectric permittivity during the heating and cooling of the sample (Fig. 4). This process is a characteristic feature of the first kind phase transitions [16,17].

The investigated samples do not demonstrate frequency dispersion of temperature of maximum dielectric permittivity as well (Fig. 5). The difference in temperature for extreme frequency values do not exceed 2K.

The temperature dependence of dielectric permittivity above the Curie temperature is described by the Curie-Weiss law. An attempt of fitting obtained data was conducted, and it turned out that the law is fulfilled only above certain T_d temperature, what leads to conclusion that the phase transition is broaden. The quantitative assessment of diffusion (γ) in the paraelectric phase was evaluated using the modified Curie-Weiss law given by Martirena and Burfoot [18]

$$\frac{1}{\epsilon} - \frac{1}{\epsilon_{\max}} = \frac{(T - T_{\max})^\gamma}{C}$$

where γ and C are constants. It is known that the value of γ ($1 \leq \gamma \leq 2$) is the expression of the diffuseness degree [19]. The formula was used to describe the temperature dependence of $1/\epsilon$ in the range of temperatures between T_C and T_d . (Fig. 6).

After applying the modified Curie-Weiss law for the measurements the γ parameter was determined, and as it was approximately the same for all the samples, equal to 1.6 what proved the conclusion made above. It is worth to note that the strontium modification does not change the diffusion of phase transition.

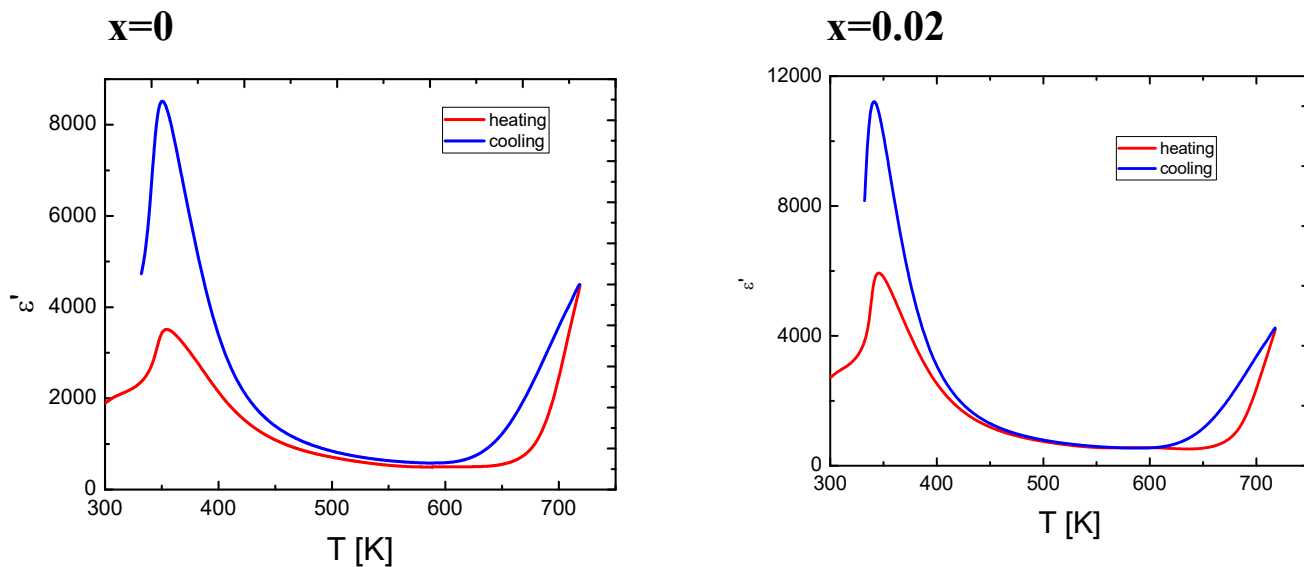


Fig. 4. Dielectric permittivity hysteresis during heating and cooling of a sample measured at frequency of measuring field equal to 1 kHz

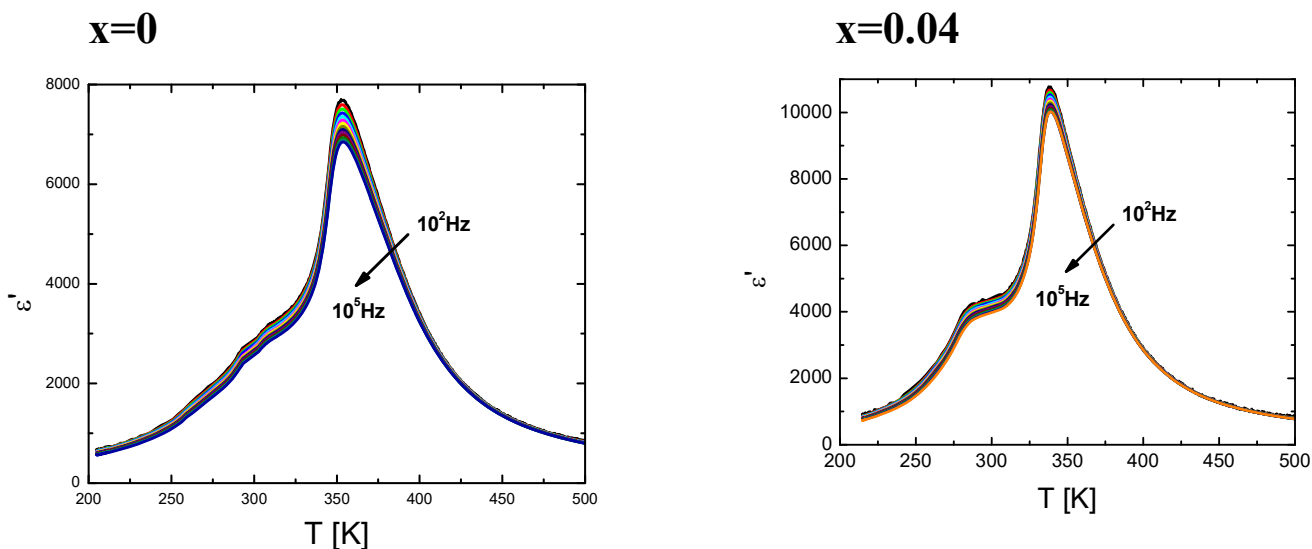


Fig. 5. Temperature dependences of dielectric permittivity for several frequencies chosen for range of 10^2 - 10^5 Hz

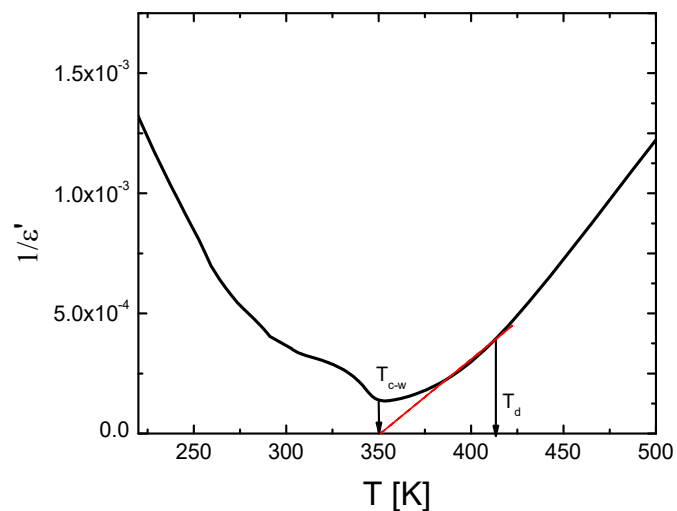


Fig. 6. Curie-Weiss temperature determination for sample containing 0.04 mol% of strontium, as example

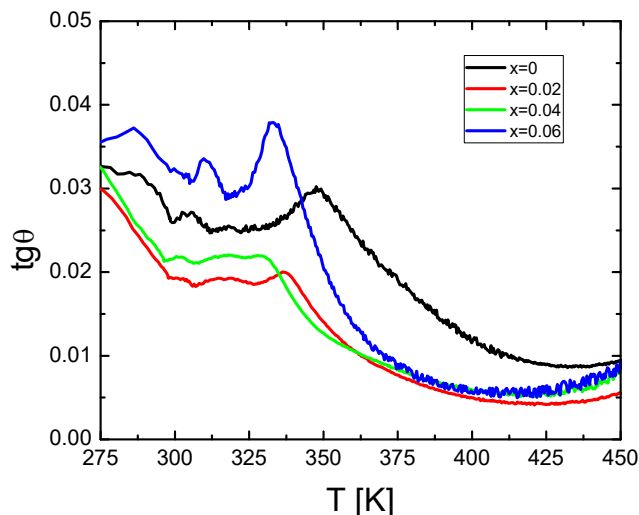


Fig. 7. Temperature dependence of loss tangent measured at frequency of measuring field equal to 1 kHz

The increase of the strontium concentration in the basic ceramics also influences the shape of temperature dependence of loss tangent, causing a change in loss tangent (Fig. 7). For the low concentrations loss tangent decreases, but for 0.06 mol% it rapidly grows. This increase is probably connected with the enhancement of the electrical conductivity of grains or grain boundaries.

It should be also emphasized that the loss tangent show a strong frequency dispersion – with an increasing measurement field it has decreased rapidly as well (Fig. 8).

3.3. Impedance spectroscopy

Impedance data was investigated as a function of temperature in the range of 473-833K and for the frequencies between 20-10⁶ Hz using a precision LCR meter Agilent E4980A. Before

further detailed analysis a coherence of obtained data had to be confirmed. Using Kramers-Kronig (K-K) validation test [20], the obtained data was confirmed compliant as the distributions of the residuals around frequency axis are random and the values do not exceed 0.5%. Results of residuals for BCZT ceramics without additives and modified by 0,04 mol% of strontium, measured at 753K, as an example, are given in Fig. 9.

The main purpose of the investigation was to determine the contribution of microstructure elements to macroscopic electric properties especially total electric conductivity. This goal was achieved by finding an adequate electric equivalent circuit (EEC) of behaviour similar to the one observed in the tested ceramics. The shape of presented on Nyquist diagram of Z' and Z'' in chosen temperatures from the range 578-758K leads to the conclusion that the impedance response comes from two different components of microstructure, as the plots have a shape of two combined semicircles (Fig. 10).

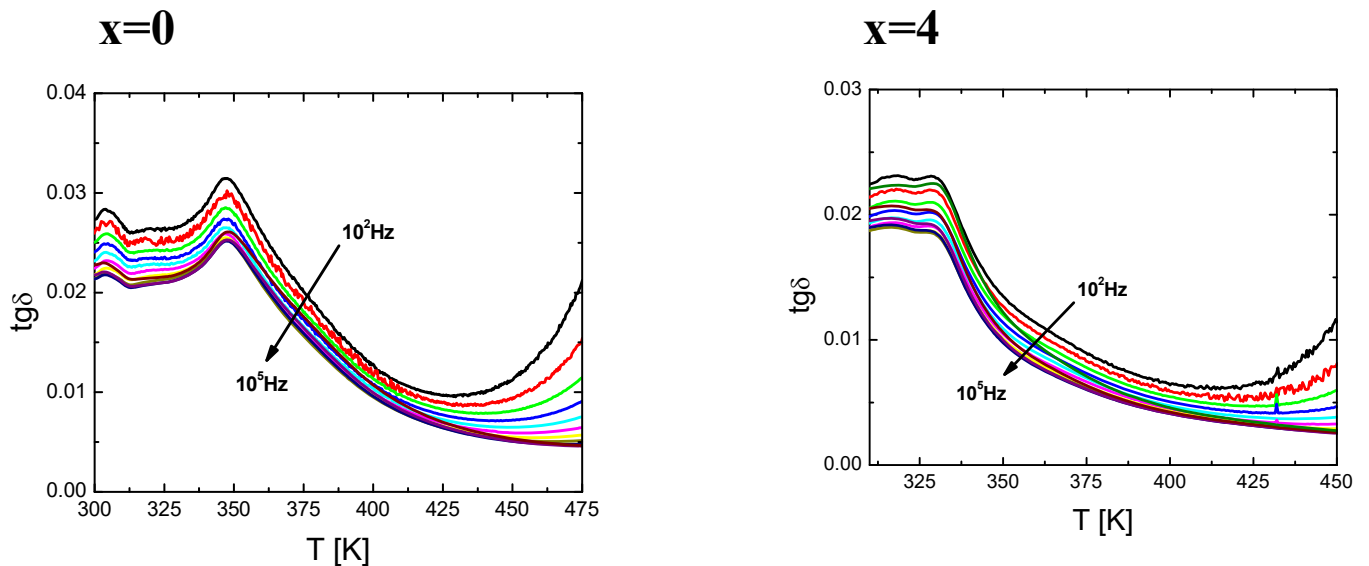


Fig. 8. Examples of loss tangent temperature dependency several frequencies chosen for range of 10²-10⁵Hz

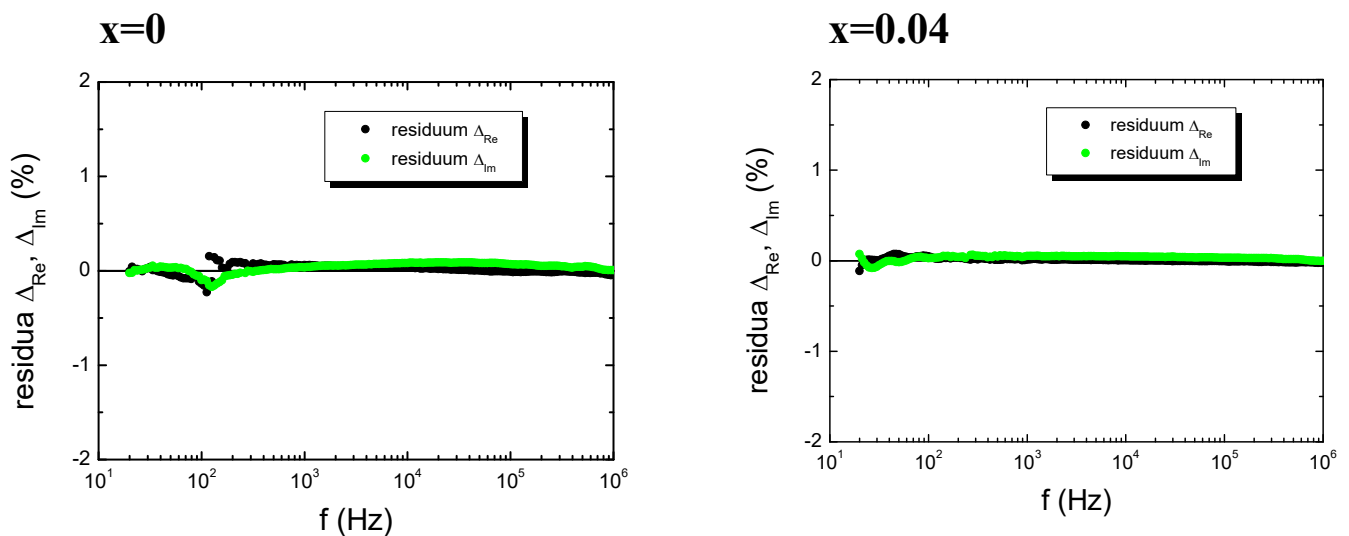


Fig. 9. Display of the Kramers-Kronig test residuals for the measured IS data of unmodified and doped BCZT ceramics as example in temperature 753K

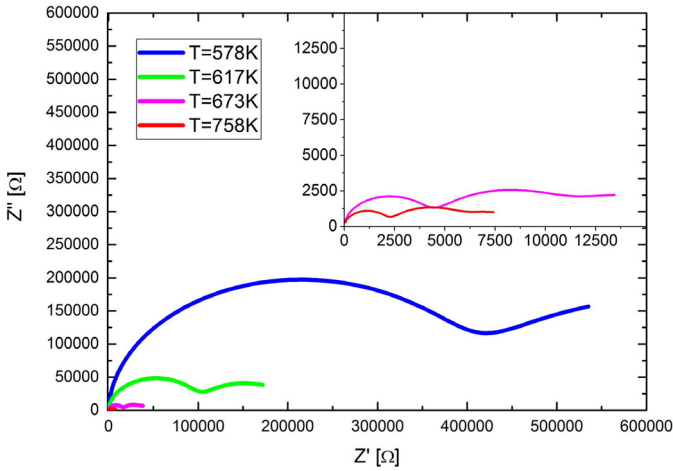


Fig. 10. Example of Nyquist diagram for pure BCZT measured in different temperatures

The consequence of these findings was selection of EEC consisting of two parallel resistance-capacitance (RC) elements connected in series, whereas the capacities were replaced with constant phase elements (CPE) (Fig. 11). This type of replacement is often practiced in the analysis of the electrical response of solids [21,22], as a CPE factor more accurately describes the behaviour of both the grains and grain boundaries.

The final step in analysing impedance spectra was data fitting to a proposed model. It was carried out by ZView equivalent circuit software produced by Scribner Associates, using complex nonlinear least square method. As a result the parameters of the material in a different temperatures were obtained. The most useful in interpretation of the processes occurring in the samples were values of resistance in grains (R_G) and grain boundaries (R_{GB}) collected in Table 2, determined at 723K.

TABLE 2

Resistance values for grains and grain boundaries for different BCZT concentrations

Sample	R_G [Ω]	R_{GB} [Ω]
$x = 0$	3838	9232
$x = 0.02$	5512	12011
$x = 0.04$	6416	14362
$x = 0.06$	6746	13388

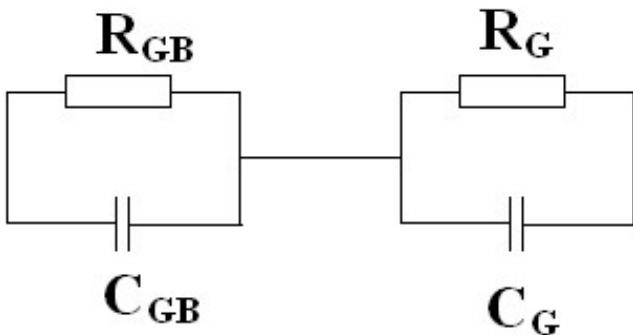


Fig. 11. Equivalent circuit used to represent the impedance response of BCZT

As it can be clearly seen with an increase of dopant concentration the resistivity of both grain and grain boundaries increase. The $\ln R_G$ and $\ln R_{GB}$ as a function of temperature have linear character, which indicates activated character of conductivity process (Fig. 12), and confirms that it might be described by a following Arrhenius formula:

$$R = R_o \exp\left(\frac{-Ea}{kT}\right)$$

The directional coefficient of linear equation allowed us to estimate the activation energy of grain and grain boundary conductivity for all of discussed samples. As it can be seen in Table 3 activation energy in grains greatly exceeds the value obtained for grain boundaries. This leads to a conclusion that the conductivity process is mostly happens trough grain boundaries both for doped and undoped BCZT. Moreover the activation energy of grains barely changes with an admixture content increases which means that used dopant have no influence on that feature. However for the grain boundaries activation energy rises significantly with a dopant concentration, leading to deterioration of conductivity in investigated ceramics materials.

TABLE 1

Values of activation energies for $(\text{Ba}_{0.85}\text{Sr}_x\text{Ca}_{0.15})(\text{Zr}_{0.1}\text{Ti}_{0.9})\text{O}_3$ ceramics for $x = 0, 0.02, 0.04$ and 0.06 mol%

Sample	E_{AG} [eV]	E_{AGB} [eV]
$x = 0$	1.13	0.85
$x = 0.02$	1.14	0.92
$x = 0.04$	1.11	0.91
$x = 0.06$	1.11	1.00

4. Conclusions

Various properties of the obtained ceramics materials were widely investigated proving good quality and novel properties of strontium doped BCZT. Especially it was confirmed that, as theoretically intended, increase in the content of strontium entails a gradual increase in the dielectric constant at T_C and linear shift towards the lower temperatures, from 344.6 to 311.3K respectively. Moreover all of the investigated samples have broaden phase transition what is confirmed by the parameter γ value. It has been proven that strontium admixture decreases loss tangent and do not show temperature hysteresis.

The impedance spectroscopy data are consistent, and indicate, that process of conductivity takes place through grains and grain boundaries. What is more the applied admixture has no influence on grains conductivity, what is shown by constant activation energy of the process, but it does decrease conductivity of grain boundaries significantly.

Taking into the consideration the presented results it could be said that the admixture of strontium improves properties of obtained ceramics material, but this effect needs further studies.

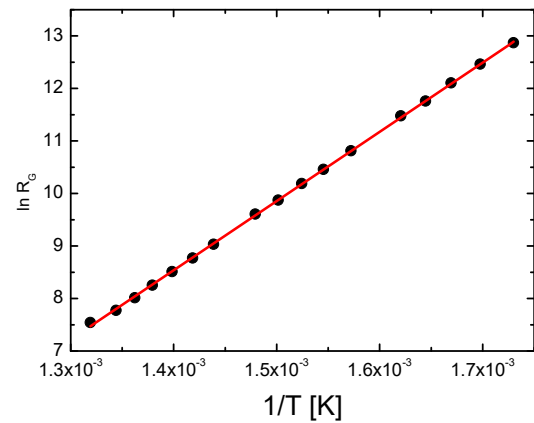
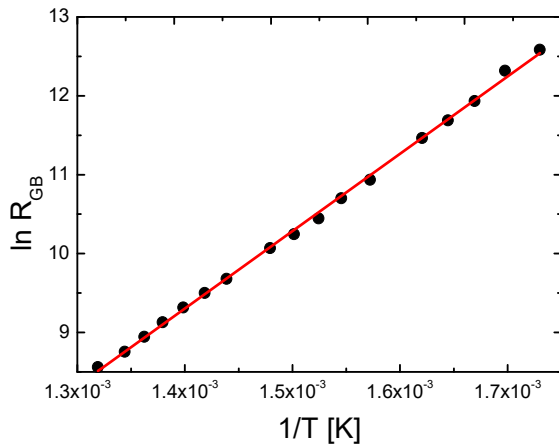
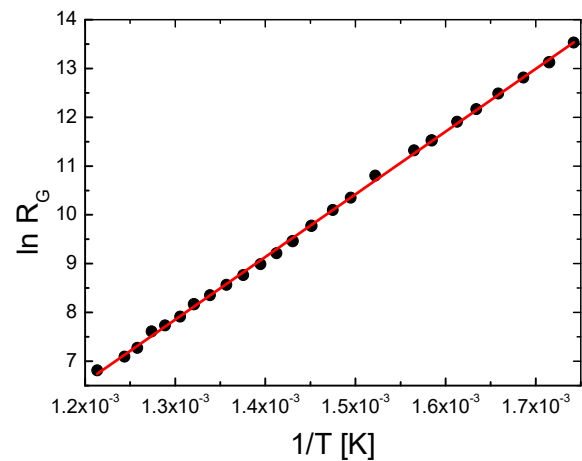
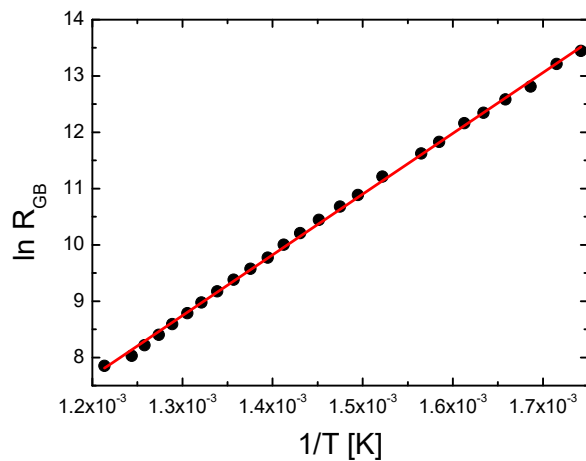
x=0**x=0.04**

Fig. 12. Examples of $\ln R_G$ and $\ln R_{GB}$ as a linear function of temperature

REFERENCES

- [1] J. Hao, W. Bai, W. Li, J. Zhai, Correlation Between the Microstructure and Electrical Properties in High-Performance $(\text{Ba}_{0.85}\text{Ca}_{0.15})(\text{Zr}_{0.1}\text{Ti}_{0.9})\text{O}_3$ Lead-Free Piezoelectric Ceramics, *J. Am. Ceram. Soc.* **95**, 1998-2006 (2012) doi:10.1111/j.1551-2916.2012.05146.x.
- [2] J. Suchanicz, Bezołowiowe tytaniany ferroelektryczne, Uniwersytet Pedagogiczny im. Komisji Edukacji Narodowej (Kraków), Wydawnictwo Naukowe, Wydawnictwo Naukowe Uniwersytetu Pedagogicznego, Kraków, 2016.
- [3] W. Liu, X. Ren, Large Piezoelectric Effect in Pb-Free Ceramics, *Phys. Rev. Lett.* **103** (2009). doi:10.1103/PhysRevLett.103.257602.
- [4] P. Parjansri, U. Intatha, S. Eitssayeam, Dielectric, ferroelectric and piezoelectric properties of Nb^{5+} doped BCZT ceramics, *Mater. Res. Bull.* **65**, 61-67 (2015). doi:10.1016/j.materresbull.2015.01.040.
- [5] C. Han, J. Wu, C. Pu, S. Qiao, B. Wu, J. Zhu, D. Xiao, High piezoelectric coefficient of Pr_2O_3 -doped $\text{Ba}_{0.85}\text{Ca}_{0.15}\text{Ti}_{0.9}\text{Zr}_{0.1}\text{O}_3$ ceramics, *Ceram. Int.* **38**, 6359-6363 (2012). doi:10.1016/j.ceramint.2012.05.008.
- [6] Y. Cui, C. Yuan, X. Liu, X. Zhao, X. Shan, Lead-free $(\text{Ba}_{0.85}\text{Ca}_{0.15})(\text{Ti}_{0.9}\text{Zr}_{0.1})\text{O}_3\text{-Y}_2\text{O}_3$ ceramics with large piezoelectric coefficient obtained by low-temperature sintering, *J. Mater. Sci. Mater. Electron.* **24**, 654-657 (2012). doi:10.1007/s10854-012-0785-7.
- [7] D. Zhang, Y. Zhang, S. Yang, Microstructure and electrical properties of tantalum doped $(\text{Ba}_{0.85}\text{Ca}_{0.15})(\text{Ti}_{0.9}\text{Zr}_{0.1})\text{O}_3$ ceramics, *J. Mater. Sci. Mater. Electron.* **26**, 909-915 (2014). doi:10.1007/s10854-014-2481-2.
- [8] H.I. Humburg, M. Acosta, W. Jo, K.G. Webber, J. Rödel, Stress-dependent electromechanical properties of doped $(\text{Ba}_{1-x}\text{Ca}_x)(\text{Zr}_y\text{Ti}_{1-y})\text{O}_3$, *J. Eur. Ceram. Soc.* **35**, 1209-1217 (2015). doi:10.1016/j.jeurceramsoc.2014.10.016.
- [9] W. Li, Z. Xu, R. Chu, P. Fu, P. An, Effect of Ho doping on piezoelectric properties of BCZT ceramics, *Ceram. Int.* **38**, 4353-4355 (2012). doi:10.1016/j.ceramint.2011.12.066.
- [10] Y.-R. Cui, X.-Y. Liu, C.-L. Yuan, X. Zhai, Y.-B. Hu, R.-W. Li, Preparation and Properties of Sm_2O_3 Doped $(\text{Ba}_{0.7}\text{Ca}_{0.3})\text{TiO}_3\text{-Ba}(\text{Zr}_{0.2}\text{Ti}_{0.8})\text{O}_3$ Lead-free Piezoelectric Ceramics, *J. Inorg. Mater.* **27**, 731-734 (2012). doi:10.3724/SP.J.1077.2012.11517.
- [12] T. Miki, A. Fujimoto, S. Jida, An evidence of trap activation for positive temperature coefficient of resistivity in BaTiO_3 ceramics

- with substitutional Nb and Mn as impurities, *J. Appl. Phys.* **83**, 1592-1603 (1998). doi:10.1063/1.366870.
- [13] R.N. Schwartz, B.A. Wechsler, Electron-paramagnetic-resonance study of transition-metal-doped BaTiO₃: Effect of material processing on Fermi-level position, *Phys. Rev. B.* **48**, (1993). doi:10.1103/PhysRevB.48.7057.
- [14] H. Herrig, R. Hempelmann, Microemulsion mediated synthesis of ternary and quaternary nanoscale mixed oxide ceramic powders, *Nanostructured Mater.* **9**, 241-244 (1997). doi:10.1016/S0965-9773(97)90063-5.
- [15] R.N. Viswanath, S. Ramasamy, Preparation and ferroelectric phase transition studies of nanocrystalline BaTiO₃, *Nanostructured Mater.* **8**, 155-162 (1997). doi:10.1016/S0965-9773(97)00004-4.
- [16] L. Zhang, L. Zhong, C.L. Wang, P.L. Zhang, Y.G. Wang, Dielectric Properties of Ba_{0.7}Sr_{0.3}TiO₃ Ceramics with Different Grain Size, *Phys. Status Solidi A.* **168**, 543-548 (1998). doi:10.1002/(SICI)1521-396X(199808)168:2<543::AID-PSSA543>3.0.CO;2-J.
- [17] N.C. Santhakumari, C.P.G. Vallabhan, Electrical conductivity, dielectric properties and phase transition in ethylenediammonium sulphate single crystals, *J. Phys. Chem. Solids.* **53**, 697-701 (1992). doi:10.1016/0022-3697(92)90210-5.
- [18] H.T. Martirena, J.C. Burfoot, Grain-size effects on properties of some ferroelectric ceramics, *J. Phys. C. Solid State Phys.* **7**, 3182 (1974). doi:10.1088/0022-3719/7/17/024.
- [19] S.J. Butcher, N.W. Thomas, Ferroelectricity in the system Pb_(1-x)Ba_x(Mg₁₃Nb₂₃)O₃, *J. Phys. Chem. Solids.* **52**, 595-601 (1991). doi:10.1016/0022-3697(91)90153-Q.
- [20] B.A. Boukamp, A Linear Kronig-Kramers Transform Test for Immittance Data Validation, *J. Electrochem. Soc.* **142**, (1995). doi:10.1149/1.2044210.
- [21] A. Lasia, Electrochemical Impedance Spectroscopy and its Applications, in: B.E. Conway, J.O. Bockris, R.E. White (Eds.), *Mod. Asp. Electrochem.*, Springer US, 2002: pp. 143-248. http://link.springer.com/chapter/10.1007/0-306-46916-2_2 (accessed September 5, 2016).
- [22] G.M. Christie, F.P.F. van Berkel, Microstructure – ionic conductivity relationships in ceria-gadolinia electrolytes, *Solid State Ion.* **83**, 17-27 (1996). doi:10.1016/0167-2738(95)00155-7.